Structural Engineering and Mechanics, *Vol. 58, No. 2 (2016) 277-300*
DOI: http://dx.doi.org/10.12989/sem.2016.58.2.277

Vibration analysis and FE model updating of lightweight steel floors in full-scale prefabricated building

Smiljana P. Petrovic-Kotur[*1] and Aleksandar P. Pavic[2a]

[1]Faculty of Construction Management, University Union Nikola Tesla, Cara Dusana 62-64, Belgrade 11000, Serbia
[2]College of Engineering, Mathematical and Physical Sciences, University of Exeter, UK

(Received September 4, 2015, Revised January 23, 2016, Accepted January 26, 2016)

Abstract. Cold-formed steel (CFS) sections are becoming an increasingly popular solution for constructing floors in residential, healthcare and education buildings. Their reduced weight, however, makes them prone to excessive vibrations, increasing the need for accurate prediction of CFS floor modal properties. By combining experimental modal analysis of a full-scale CFS framed building and its floors and their numerical finite element (FE) modelling this paper demonstrates that the existing methods (based on the best engineering judgement) for predicting CFS floor modal properties are unreliable. They can yield over 40% difference between the predicted and measured natural frequencies for important modes of vibration. This is because the methods were adopted from other floor types (e.g., timber or standard steel-concrete composite floors) and do not take into account specific features of CFS floors. Using the adjusted and then updated FE model, featuring semi-rigid connections led to markedly improved results. The first four measured and calculated CFS floor natural frequencies matched exactly and all relevant modal assurance criterion (MAC) values were above 90%. The introduction of flexible supports and more realistic modelling of the floor boundary conditions, as well as non-structural façade walls, proved to be crucial in the development of the new more successful modelling strategy. The process used to develop 10 identified and experimentally verified FE modelling parameters is based on published information and parameter adjustment resulting from FE model updating. This can be utilised for future design of similar lightweight steel floors in prefabricated buildings when checking their vibration serviceability, likely to be their governing design criterion.

Keywords: vibration analysis; FE model updating; lightweight steel floor; prefabricated building

1. Introduction

The prefabrication and preassembly of building components are recognised as major breakthroughs in the construction industry all over the world, especially when the improvement of quality, productivity, and energy efficiency is concerned (Egan 1998, NRC 2009, Timetric 2014). The value of the global prefabricated buildings market was US$90.1 billion in 2012 and the

∗Corresponding author, Research Associate, E-mail: spetrovic.fgm@gmail.com
[a]Professor, E-mail: a.pavic@exeter.ac.uk

http://www.techno-press.org/?journal=sem&subpage=8 ISSN: 1225-4568 (Print), 1598-6217 (Online)

expected annual growth rate is a very admirable 8.6% for the period 2013-2017 (Timetric 2014). The use of prefabrication and modularisation is no longer related exclusively to commercial and industrial building applications, as they are increasingly popular in the health, education, and housing construction markets (Hartley and Blagden 2007, Cowles and Warner 2013).

Cold-formed steel (CFS) products have traditionally been used for non-structural prefabricated assemblies, such as cladding, partition walls and roof panels. More recently, there is an apparent trend of their implementation in the structural frames of low- and medium-rise residential buildings. Light CFS load-bearing frames and floors are found to be the best substitution for the conventional wood frames of houses in seismic areas, such as Japan and the western parts of the United States, and in warm, humid areas where wood structures are exposed to termite infestation or susceptible to mould (Lawson *et al.* 1999, Mehta *et al.* 2013).

The advantages of using CFS structural components are numerous, one of the most important ones being fast construction and considerably lower mass. However, their light weight means that CFS framed floors may exhibit excessive vibrations induced by everyday human activities, typically walking.

The term 'CFS framed floors' refers to a grid of CFS joists and beams, forming a support for a deck, which can be in the form of plywood, chipboard, oriented-strand board (OSB), corrugated metal sheathing, lightweight or composite concrete slab. They are also termed 'lightweight steel floors' due to the low overall structural floor weight (150 kg/m^2 or less). It should be noted that, when the floor decking has relatively low local bending stiffness (e.g., chipboard and OSB), a notable static-like deflection is caused by the sheer force of each footstep. These deflections have local character and mainly affect the person who causes and feels them due to springiness (Ohlsson 1982).

Interestingly, despite this phenomenon, caused by the low stiffness of the decking, the CFS framed floors, along with timber floors, are normally behaving as so called 'high-frequency floors' (HFF) (Kesti *et al.* 2008). This indicates that the overall floor structure is quite stiff, having vibrations due to walking dominated by a series of transient responses following each footstep. The fundamental frequency of HFFs is above a certain threshold, which varies from 7 Hz to 12 Hz, depending on the design guidance used (Wyatt 1989, Pavic and Willford 2005, Willford and Young 2006). However, the higher strengths and longer spans of CFS floor beams, compared to timber floor beams, yield lower fundamental frequencies, which are often below 10 Hz. As will be seen later, the experimental investigation presented in this paper demonstrates that, even if the fundamental frequency of the lightweight steel floor is below 10 Hz, the floor response can still be dominated by the high-frequency transient rather than low-frequency resonant response character. This phenomenon was previously observed by Pavic *et al.* (2008), but for *beam and block* rather than CFS floors.

Vibration serviceability of CFS floors is characterised by many uncertainties, particularly when FE modelling and calculation of the modal properties are concerned. When CFS framing first made its way into the construction industry, buildings were constructed following many of the practices used in wood framed structures. The analogy between CFS and wood frames has been reflected in CFS design approaches. It still persists in vibration analyses of CFS floors, despite the considerable differences in vibration response magnitudes, dissimilarities in mechanical properties of wood and steel, and the behaviour of connections. The alternative design approach is to apply the vibration serviceability modelling guidelines pertinent to standard hot rolled steel (HRS) framed floors. This practice relies on evident similarities in material properties and connections, but neglects the great difference in mass and levels of vibration response. None of the modelling strategies considers the unique features of the CFS framing structures.

Connections are an important aspect of structural behaviour. While the introduction of semi-rigid connections in analytical/numerical models in static analysis is widely encouraged and supported by systematic design procedures, a general rule in vibration analysis of the standard composite HRS and concrete floors is that all joints should be modelled as rigid (Pavic and Reynolds P. 2002). This is because strains due to vibration displacements are so small that even friction in joints cannot be overcome. On the other hand, investigations related to timber floors suggest that the stiffness of the connections should be taken in account when modelling vibration behaviour, because wood always deforms around the embedded fastener (Leichti *et al.* 2000, Reynolds T. *et al.* 2014). The key question is how CFS connections behave.

This paper therefore presents a combined experimental and analytical study concerned with modal analysis of lightweight steel floors, in which modelling CFS connections plays a crucial role. The review of the literature pertinent to vibration performance of CFS framed floors is presented in the second section. A description of the test structure is given in Section 3. The results of a multi-input-multiple-output (MIMO) modal testing carried out on the first floor of a two-storey prefabricated building can be found in Section 4. Finally, Section 5 covers experimentally verified FE modelling assumptions pertinent to a full-scale CFS test floor, which can be used for future design of similar structures.

2. Literature review

CFS and timber framed floors are commonly referred to as 'lightweight floors', while standard concrete and HRS framed floors are considered 'normal weight' or sometimes 'heavy' floors (Hu *et al.* 2006, Ljunggren 2006, IBC 2012). Ohlsson (1982) defined a lightweight floor as one where the presence of a human significantly alters the floor modal parameters. However, the amount of change in the modal properties caused by a 'typical' human was not quantified. It was also stated that floors with modal masses higher than 1,000 kg (using unity-scaled mode shapes) in all relevant modes should be considered heavy floors.

The liveliness of the lightweight floors was detected a long time ago and it has been mainly associated with timber floor structures. Consequently, the majority of the literature relevant to the vibration serviceability of lightweight floors deals with timber floors. The following review comprises references related to timber floor vibrations dealing with the incorporation of semi-rigid connections in analytical/FE models. It also includes investigations pertinent to the vibration analysis of CFS floors, with an emphasis on analytical/FE modelling.

Many researchers (Gupta 1985, Chui 1988, Filiatrault *et al.* 1990, Hu 1992) have developed mathematical models of timber floors involving semi-rigid connectors at the decking-joist interface. Hu *et al.* (2002) and Jiang *et al.* (2004) established special connector elements to model the semi-rigid connections between joists and lateral reinforcement members (e.g., strong back or bridging), as well as semi-rigid connectors at the flooring-joist interface. The static deflections were found to be well predicted by the model, while the fundamental frequencies were generally over-predicted. The explanation for this was that the end supports of the joists were modelled as rigid. However, a good agreement of the test and FE static deflections, and an overestimation of the measured fundamental frequency by the same FE model can imply that connection stiffness is different, depending on whether the floor is statically loaded or it is dynamically excited.

References concerning the vibration serviceability of CFS floors (Kraus 1997, Tangorra *et al.*

2002, Xu and Tangorra 2007, Parnell 2008, Parnell *et al.* 2010, Xu 2011) comprise extensive experimental research conducted in laboratories and on in-situ floors. Analytical investigations are mostly limited to comparisons of measured floor responses, both static and dynamic, to design limit values defined in design codes pertinent to timber and HRS floors. Kraus (1997), Tangorra (2002) and Parnell (2008) conducted additional studies where certain parameters (fundamental frequency, static deflection etc.) were calculated following procedures suggested in some design guidelines and compared with the measured values. In Parnell's (2008) study the best correlation was obtained following recommendations given by the ATC design guide (Allen *et al.* 1999) where the standard deviation of error for the in-situ measured fundamental frequency of the floor was quite high, at 16% (min. error is 1%, and max. is 36%). For the laboratory floors, it was even higher, at 44% (min. error is 19%, and max. is 83%). The very poor matching between the measured and calculated natural frequencies indicates that the analytical procedures proposed in design guides related to timber and HRS floors, as well as in the ATC guide (Allen *et al.* 1999), which includes lightweight steel floors, may not be reliable when estimating the modal properties of CFS floors.

Zhao *et al.* (2003) investigated the influence of connection stiffness on the fundamental frequency of a DuraGal floor. Joists, bearers and piers were rectangular hollow CFS sections and particleboard was used for the flooring. It was found that the *shear* stiffness of the joist-to-beam connection drastically altered the fundamental frequency of the grillage model, which represented the tested floor. Shear connections between particleboard and joists, rotational stiffness of the joist-to-beam connections and rotational stiffness of the beam-to-column connections had negligible effects. These results do not completely represent the actual dynamic stiffness of the floor, since they were obtained for the fundamental frequency only. Namely, the fundamental mode engaged in bending mostly the main beams to which joists are framed at the right angle. Therefore, the joists were not engaged in bending, so the rotational stiffness of joists and their connections did not affect the fundamental frequency. The influence of joist stiffness increases in higher modes where they get engaged more in bending, thus the influence of the joist-to-beam and deck-to-joist connections also increases in higher modes. Considering the transient multi-mode response character of the CFS floor vibrations, the contribution of higher vibration modes must be accounted for. Therefore, a good correlation between measured and calculated higher modes is crucial for the validation of the proposed FE model.

In addition, Zhou *et al.* (2011) developed an FE model of a CFS concrete composite floor, with semi-rigid connections to analyse its vibration behaviour. Good agreement between the test and FE model results was achieved, but for the fundamental frequency only.

Rack and Lange (2009) reported results and observations obtained during the dynamic testing of lightweight steel floors made in a laboratory. Although some recommendations for the modelling of CFS framed floors are given, calculated natural frequencies and mode shapes for the tested floors were not presented in the paper. However, it is worth mentioning that the paper suggested introducing springs (both rotational and translational) at the deck-joist interface. In addition, the experimenters realised that the substitution of screws (between flooring and joists) by a nailing system with higher shear stiffness had different effects on the measured static deflection and accelerations. This implied different connection behaviour depending on whether static or dynamic loading was used in the CFS floors.

In conclusion, the literature review revealed that there is a need for focused research specifically into CFS floor vibration behaviour. Particular emphasis should be on the modelling of typical CFS floor connections pertinent to their vibration behaviour, as opposed to static behaviour.

3. Description of test structure

A full-scale prototype building (comprising two prefabricated modules) was built to conduct modal testing to experimentally estimate its modal properties (Fig. 1). Each module has a rectangular 3.3 m×12 m plan and two storeys (ground and first floor), with a height of approximately 3.5 m. Four columns, positioned at the corners of each module, support the 12 m long main beams at the ground and first floor and the roof (Fig. 2).

Fig. 1 External view of the two-module prototype test building

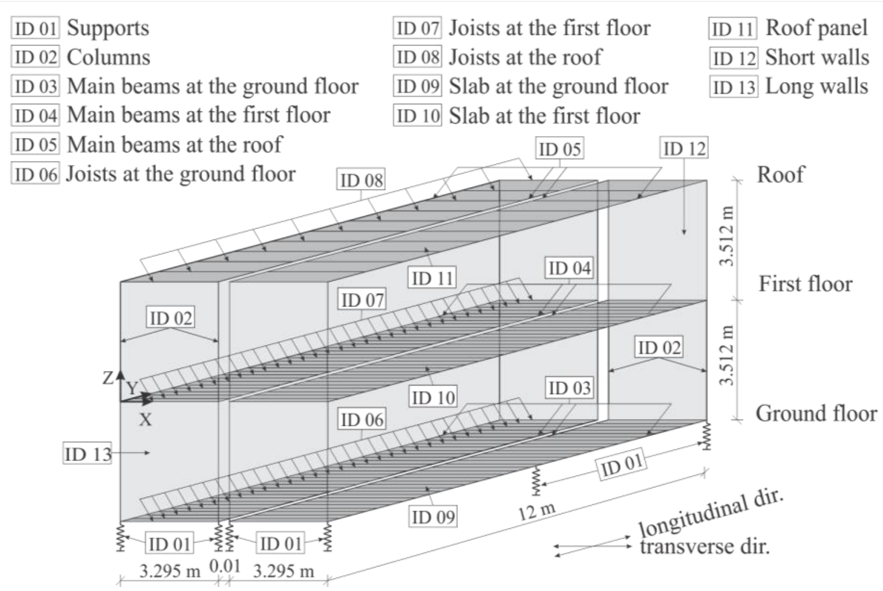

Fig. 2 Structural scheme of the test building

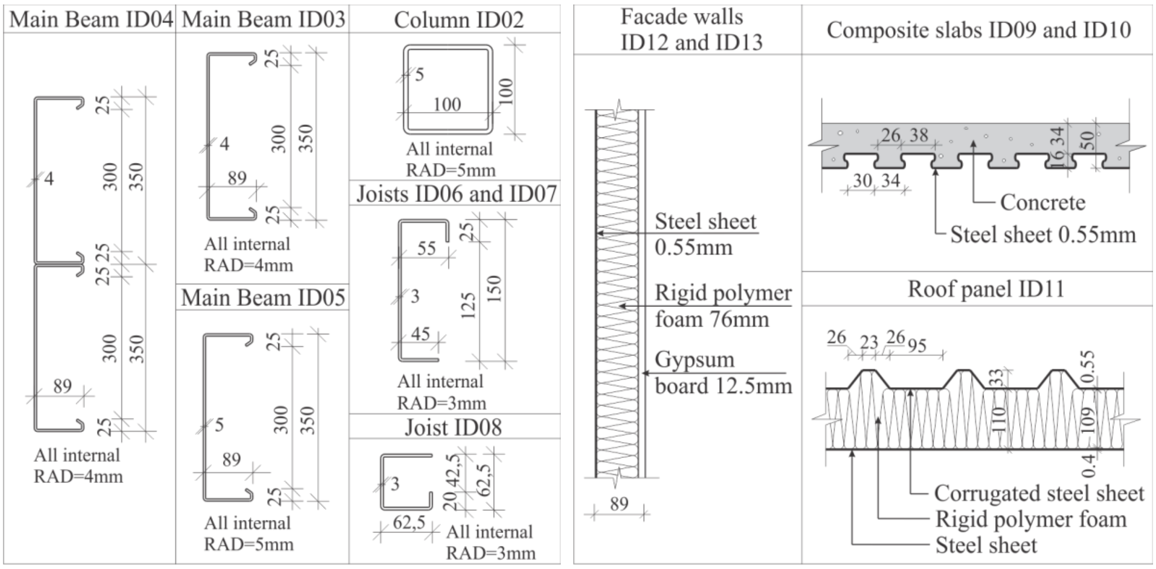

(a) Columns, main beams, and joists (b) Façade walls, composite slabs, and roof panel

Fig. 3 Cross sections

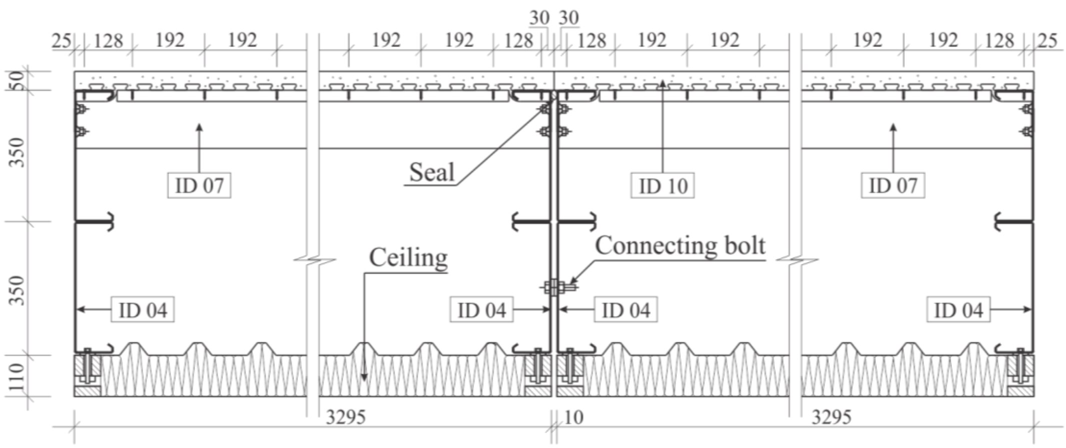

Fig. 4 Cross section of the first floor

Joists span 3.3 m in the direction orthogonal to the main beams and they are spaced at 0.2 m each at the first and the ground floor, and at 1.2 m each in the roof. Columns, main beams and joists are CFS members and their cross-sections are shown in Fig. 3(a). A lightweight composite slab, comprising profiled steel decking with in-situ cast concrete topping, is supported by a steel frame at the first and the ground floor. A non-structural roof panel rests on the steel frame at the top of the building. The façade consists of sandwich panels. Cross-sections of the composite slab, roof panel and façade wall are depicted in Fig. 3(b). The same type of sandwich panel used for roofing was also utilised for the ceiling connected to the bottom flanges of the main beams at the first floor (Fig. 4). The mass of the floor was as low as 150 kg/m^2.

Two prefabricated modules are connected, at all three levels, by bolts at nine equidistant collinear points connecting pairs of main beams (Fig. 4). This is the standard way of connecting modules (Lawson *et al.*1999). Ten footings (eight under the columns and two at the mid-span of the outer main beams of the ground floor, Fig. 2) are made of rectangular hollow steel sections (insert in Fig. 1) and placed on the ground. They are not fixed to the ground or the structure in any way. Testing was conducted on the bare structure, without partitions and furnishings.

4. Modal testing

MIMO modal testing was conducted on the full-scale 2-module prototype building described in the previous section. All measurements were carried out on the first floor. To perform modal testing, a test grid was developed, comprising 25 test points (TPs), as shown in Fig. 5, with accelerometers measuring vertical acceleration. The vertical excitation of the floor structure was provided by two APS Dynamics Model 113 electrodynamic shakers, placed at TP9 and TP12 (Fig. 5). People and equipment for data acquisition were placed at the floor corner to minimise their influence on the floor mass and damping. Modal testing methodology was in accordance with recommendations by Reynolds P. and Pavic (2000).

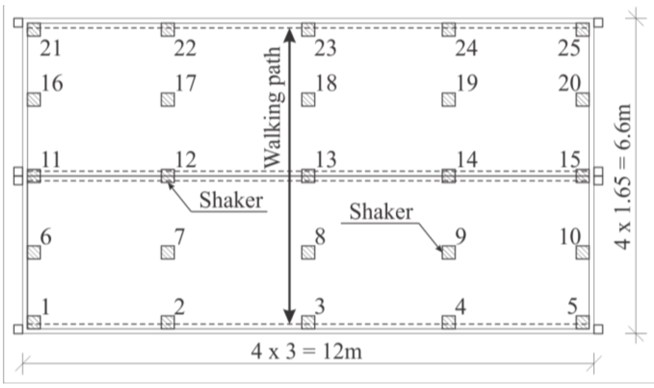

Fig. 5 The 25-point test grid used in MIMO testing of the first floor

A set of 50 frequency response function (FRF) moduli, corresponding to two reference locations (input points TP9 and TP12) in the range of 0.5 to 50 Hz is shown in Fig. 6(a). FRF curves corresponding to TP9 (blue lines) and measured at points from TP6 to TP10 (Fig. 5) have higher peak amplitudes in the frequency range above 20 Hz, indicating that local modes were dominant in their acceleration response. Fig. 6(b) shows the reciprocity check (Ewins 2000) between FRFs corresponding to TP9 and TP12. For a structure that behaves linearly, these two curves should theoretically be identical, due to the Maxwell's reciprocity theorem. However, in practice, they always differ due to inherent noise and nonlinearities in real structures. It can be seen that there is a better agreement between FRFs for frequencies below approximately 20-25 Hz than for the frequencies above this value, indicating possible non-linear behaviour related to localised high-frequency modes with low modal mass.

All FRFs pertinent to TP 9 were curve-fitted in the ME'scope software (Vibrant Technology 2003). Fig. 7 shows the estimated modal properties for the lowest four vibration modes. It can be

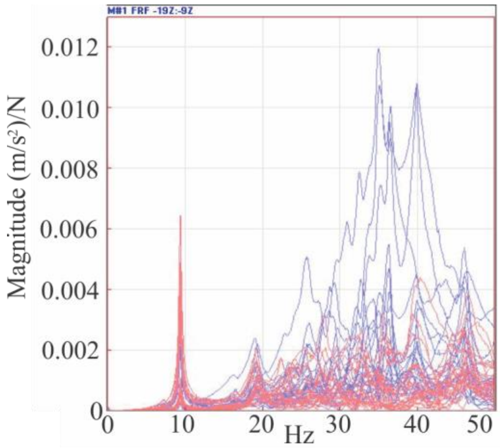

(a) All measured FRFs between 0.5 and 50 Hz

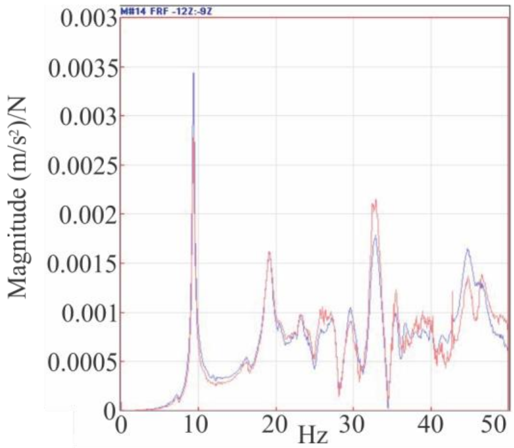

(b) Reciprocity check between TP9 and TP12

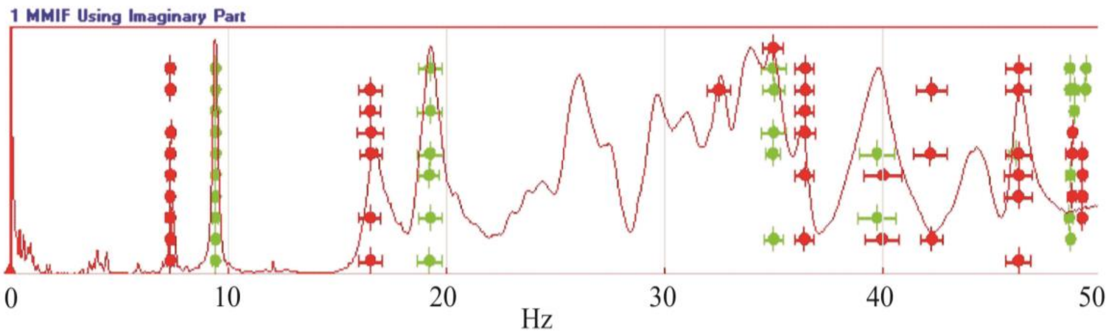

(c) Stability diagram

Fig. 6 FRF moduli

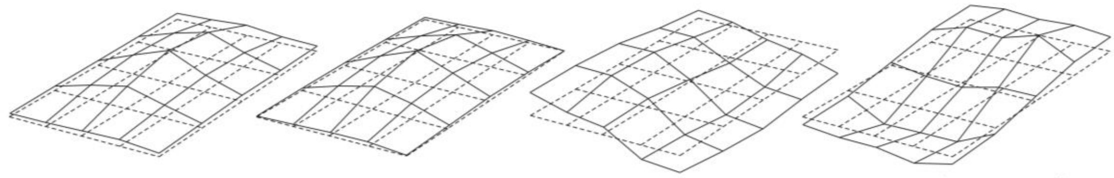

Mode 1: f1=7.43Hz; ζ1=1.0% **Mode 2**: f2=9.41Hz; ζ2=1.4% **Mode 3**: f3=16.26Hz; ζ3=2.2% **Mode 4**: f4=19.24Hz; ζ4=3.1%

Fig. 7 Modal properties estimated by curve-fitting

seen that none of the first four modes have a local character. It was decided that only FRF curves corresponding to TP9 for curve-fitting would be used, because the third mode could not be clearly observed and extracted if all FRFs were used. It was concluded that the shaker placed on the main beam (TP12) could not properly excite the third mode (Fig. 7) because the main beam lies on the nodal line of this mode. In addition, the stability diagram shown in Fig. 6(c) clearly confirms that the modes estimated by curve-fitting are the only four stable modes in the frequency range of interest (0-25 Hz). Differences between the natural frequencies of the first four modes obtained by curve-fitting and the corresponding ones determined by the stability diagram were negligible.

At first sight, the first two modes in Fig. 7 look almost the same, but - in fact - there is a

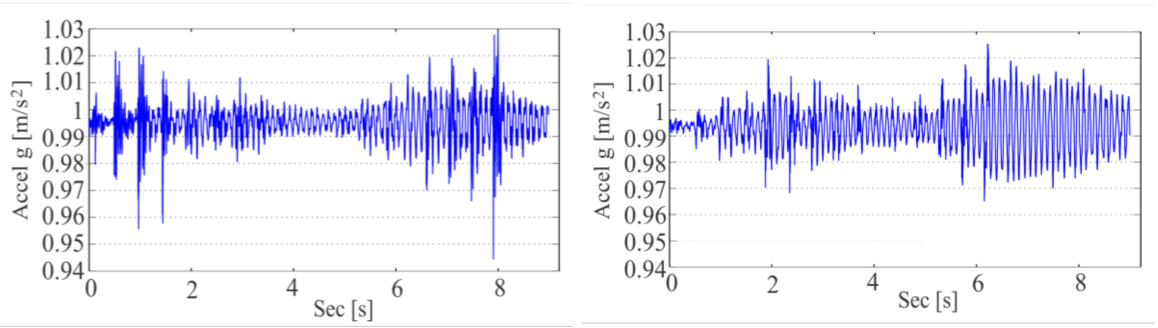

(a) at TP8 (b) at TP13

Fig. 8 Walking responses

considerable difference between them. Namely, vertical motion along the floor edge and especially at the four corners is larger in the first than in the second mode. This implies that the first mode possibly engages the whole building, while the second mode is mostly confined to the first floor level. Large vertical motion along edges and at corners is highly visible in the third and fourth mode too. Hence, it is reasonable to assume that the whole building structure is also engaged in these modes. In conclusion, there are three 'global' modes and one 'local' mode, where the term 'global' relates to whole building motion, and 'local' corresponds to the first floor structure. Moreover, the second experimentally estimated mode (Fig. 7) will be called 'fundamental mode of the first floor' as it is dominated by the motion of the first floor. The frequency of this mode is 9.41 Hz and it relates to the first clear peak observed in the FRF set.

The damping ratios estimated by curve-fitting (Fig. 7) were compared to the ones obtained by the stability diagram. Differences were small for the second (1.4% vs. 1.3%) and the fourth mode (3.1% vs. 3.0%), but they were considerably high for the first (1.0 vs. 2.4%) and the third mode (2.2% vs. 3.2%). The damping values estimated by the stability diagram were regarded as more reliable. The lowest damping value of 1.3% was obtained for the second mode, which was referred to as the 'local' mode. Apparently, the vertical motion of the whole building in the 'global' modes caused the greater loss of the vibration energy.

Fig. 8 shows the vertical accelerations due to walking measured at 2 locations: TP8 (located at the subfloor between main beams) and TP13 (placed at the main beam). The test subject walked at 2.35 Hz along the walking path depicted in Fig. 5 (from TP3 to TP23 and back). It is important to note that the fourth harmonic of the 2.35 Hz walking force resonates at approximately 9.41 Hz, which corresponds to the second measured mode. The response measured at TP8 has apparent transient peaks and it is most likely governed by the higher modes developing between the main beams. The acceleration response measured at TP13 is made of smaller transient and relatively greater steady-state responses, as would be expected for a point on the main beam. Evidently, the classification into either low- or high-frequency floor type is not applicable to this CFS floor, as its vibration response is a combination of both considerable resonant and transient components. This emphasises the need for reliable FE modelling able to capture multi-modal low- and high-frequency responses.

5. FE modelling

An FE model of the investigated prefabricated building was developed using ANSYS FE code (Ansys Inc. 2005) to calculate its modal properties. In particular, an FE model of the whole building was developed for two reasons:

- the experimental results indicated that there were three global modes of the whole building that affected vibrations of the first floor (modes 1, 3, and 4 in Fig. 7), and
- it was the most appropriate way to model the first floor boundary conditions.

5.1 General assumptions

Best engineering judgement was employed in the development of the FE model, using assumptions that are common in design practise when performing vibration serviceability checks (Pavic and Reynolds 2002). All materials were assumed to be linearly elastic. Structure imperfections, such as non-uniform dimensions of the elements along the length or over the area, uneven mass distribution, etc. were neglected. All connections were modelled as rigid, because it was assumed that the structural deformation during modal testing was so small that friction in the joints was not overcome (Kesti *et al.* 2008). The non-structural elements, such as exterior walls and roofing, were incorporated explicitly in the model, because modal testing results indicated that they could considerably affect the modal properties of the structure.

Columns, joists and beams (all one-dimensional structural elements) were represented in the model by 3D beam elements (BEAM4). Cross-section data (area, moment of inertia, torsional moment of inertia, etc.) for all 3D beam elements were determined based on the geometry obtained from structural drawings (Fig. 3(a)). The characteristics of all the materials are listed in Table 1. Composite action was assumed for all elements featuring steel beams and a concrete slab, with the neutral axis assumed at the interface of the two. According to El-Dardiry and Ji (2007) natural frequencies are not particularly sensitive to changes of the common neutral axis position, as long as it is reasonably assumed.

Both floors, roof and walls were modelled using SHELL63 elements. When modelling the composite slab (ID09 and ID10, Fig. 3(b)) using SHELL63, a procedure proposed by El-Dardiry and Ji (2006) was used to determine the shell thickness and 'equivalent' Young's moduli of elasticity in the two orthogonal directions, assuming constant SHELL63 thickness. The end result was that the elements had a thickness of 0.023 m and the Young's moduli were Ey=210 GPa and Ex=1.357*Ey. Similarly, the sandwich roof panel (ID11, Fig. 3(b)) had a thickness of 0.033 m and the Young's moduli were Ey=210 GPa and Ex=1.902*Ey. Finally, exterior walls (ID12 and ID13, Fig. 3(b)) were assumed to be isotropic shells with a thickness of 0.0125 m and Ey=Ex=10.96 GPa.

As the first floor was very light, masses of the two shakers were included as MASS21 elements concentrated at the nodes corresponding to TP9 and TP12 positions (Fig. 5). The masses of the

Table 1 Materials

Material	Density [kg/m^3]	Young's modulus of elasticity [Pa]
Concrete	2350	2.9E+10
Steel	7850	2.1E+11
Gypsum	900	1.5E+09
Rigid Polymer Foam	40	3.0E+07

people present on the floor during modal testing and of the equipment were added to the mass of the shell elements on the first floor (a total of 200 kg 'smeared' over the whole floor area). The ceiling connected to the beams supporting the first floor was assumed to add only mass and no stiffness to the first floor (Fig. 4). The two building modules were connected only by short beam elements (BEAM4), simulating bolts along the main beams at the all three levels. Supports were represented by vertical springs (COMBIN14) due to the vertical motion of the whole building observed in the experimental results (Section 4). Horizontal displacements of the columns and façade walls were restrained.

The total number of elements used in FE modelling is 64,348 (SHELL63-53,341; BEAM4-10,995; COMBIN14-10; and MASS21- 2).

A modal analysis using ANSYS software was performed utilising the Lanczos eigenvalue extraction algorithm. A validation of the FE model was carried out in correlation with experimental modal data. Mode pairing was established using the Modal Assurance Criterion (MAC) (Allemang and Brown 1982).

5.2 Model improvement

Model improvement had two phases:

• model updating (manual and automatic), and
• model adjustment.

5.3 Model updating

A sensitivity-based model updating technique (Friswell and Mottershead 1995) in the design optimisation module of the ANSYS FE code was used to improve the correlation between the computed and measured modal data. The objective of the model updating process was to minimise the error function based on the differences between the measured and calculated natural frequencies. The correlation between mode shapes quantified by MAC was chosen to pair the modes. MAC values were not included in the error function, because they were not very sensitive to the parameter changes. This is in agreement with the approach to model updating reported by Sinha and Friswell (2002).

The FE model updating process had three phases: 1) a sensitivity study 2) manual model tuning, and 3) automatic model updating. The aim of the sensitivity study was to identify the most uncertain parameters and to analyse their influence on the natural frequencies. The study was performed using the *gradient evaluation tool* in ANSYS. The finite differential approach (Friswell and Mottershead 1995) was applied, in which the updating parameters had been increased by only 1%, due to a highly non-linear dependence of the natural frequencies on the changes of the updating parameters. Based on the results of the sensitivity study, the parameters with the greatest impact on the natural frequencies were selected for the manual model tuning. As low as possible number of parameters is a crucial prerequisite for a well-conditioned model updating process. To overcome the large differences in the natural frequencies and to accelerate the subsequent automatic model updating procedure, it was necessary to apply manual model tuning, where the user defines the parameter changes in every iteration. The automatic updating process would either not converge, or would converge very slowly without the prior manual tuning. This problem was recognised by Brownjohn and Xia (2000). The so called *first order method* in ANSYS was used for automatic updating. Although this method is the most accurate one (Ansys Inc. 2005), it is also quite time consuming. Therefore, the minimal number of parameters was chosen to make the process most effective. The error function given in Eq. (1) was defined as a weighted sum of the squared differences of the four natural frequencies selected as targets for updating

$$J(\theta) = \sum_{i=1}^{4} \left(\frac{f_{ei} - f_{ci}(\theta)}{f_{ei}} \right)^2 \tag{1}$$

where $J(\theta)$ is the error function, f_{ei} and $f_{ci}(\theta)$ are the *i*th experimental and computed natural frequencies, respectively, and θ is the vector of the parameters being updated. The difference between the measured and calculated natural frequencies was weighted by the inverse of the experimental natural frequencies f_{ei} to normalise the contribution of every mode to the total error $J(\theta)$. Batch processing was used for the creation of the FE model and later optimisation process. The error function was defined as a parameter which was minimised. MACs were calculated for different pairs of measured and FE modes. If the MAC value was above 0.7, the corresponding pair of modes was used for calculating the difference in natural frequencies, and consequently the calculation of the error function. The pairing of the first two calculated modes with the measured counterparts was not conditioned by MACs, since they have never changed the sequence.

5.4 Model adjustment process

As will be seen later, after the initial manual and automatic model updating exercises, it became clear that considerable additional changes in the connections (assumed to be rigid) of the FE model were needed. The model was *adjusted* by an introduction of semi-rigid joints. MATRIX27 was chosen as the most suitable element. It is an arbitrary element defined by two nodes and coefficients representing its own stiffness, mass or damping matrix. Hence, it can be used to represent a structural, a damper or a mass element.

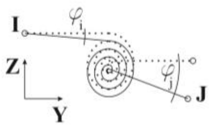

$$\begin{vmatrix} C & -C \\ -C & C \end{vmatrix} \cdot \begin{vmatrix} \varphi_i \\ \varphi_j \end{vmatrix} = \begin{vmatrix} M_i \\ M_j \end{vmatrix}$$

UX	UY	UZ	ROTX	ROTY	ROTZ	UX	UY	UZ	ROTX	ROTY	ROTZ	
1E+15	0	0	0	0	0	-1E+15	0	0	0	0	0	UX
	1E+15	0	0	0	0	0	-1E+15	0	0	0	0	UY
		1E+15	0	0	0	0	0	-1E+15	0	0	0	UZ
			C	0	0	0	0	0	- C	0	0	ROTX
				1E+15	0	0	0	0	0	-1E+15	0	ROTY
					1E+15	0	0	0	0	0	-1E+15	ROTZ
						1E+15	0	0	0	0	0	UX
							1E+15	0	0	0	0	UY
			SYMMETRIC					1E+15	0	0	0	UZ
									C	0	0	ROTX
										1E+15	0	ROTY
											1E+15	ROTZ

Fig. 9 Stiffness matrix of the main beam-to-column joint given in the global coordinate system XYZ

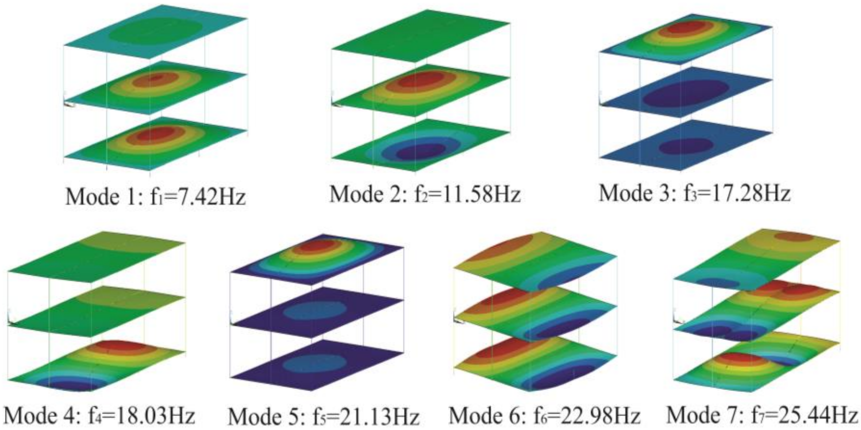

Fig. 10 First seven modes of vibration determined by initial FE model (Model 1)

The stiffness matrix of the joint, which provides rotation only about the x-axis, is depicted in Fig. 9 where C is the rotational stiffness, and φ_i and φ_j are rotations in the vertical plane of the *i*th and *j*th nodes. Elements at the main diagonal of the presented matrix are the stiffness of the remaining DOFs of the joint. They should be large enough to prevent relative displacement between the nodes and they were assumed to be 10^{15} N/m and 10^{15} Nm/rad for displacements and rotations, respectively. The mass and the damping features of the joint were neglected.

The total number of elements in the improved FE model was 68,105 (SHELL63-51,800, BEAM4-11,157, COMBIN14-10, MASS21-2, MATRIX27-5,136).

5.5 Results

This section presents the results of initial FE modelling (Model 1) and subsequent model adjustment (Model 2).

5.5.1Initial FE model - Model 1

The first seven FE modes of Model 1 are presented in Fig. 10 (walls are omitted for clarity). Comparing the mode shapes depicted in Fig. 7 and Fig. 10, it can be seen that the first and second numerically calculated modes correspond to the first and second experimentally estimated modes, respectively. The sixth mode of Model 1 relates to the third measured mode, and the seventh FE mode relates to the fourth measured mode. The developed FE model overestimates the natural frequencies for all test modes except the first one. The greatest difference, of approximately 41% between numerically predicted and measured natural frequencies, is observed for the third test mode (16.26 Hz measured vs. 22.98 Hz calculated).

It should be mentioned that the third and fifth mode of Model 1 (Fig. 10) are dominated by the vibrations of the roof. Also, the fourth FE mode mostly engages the ground floor. The shakers placed at the first floor probably could not excite these modes, so it was not possible to estimate them from the experimental results.

Nevertheless, it can be seen that the application of the best engineering judgement resulted in significant discrepancies between the measured and calculated natural frequencies. This indicates that there are features in the FE model that require significant changes, confirming the hypothesis of this paper that there is a need for better understanding of the dynamic behaviour of CFS floors.

Considering the differences between the calculated and measured natural frequencies, a sensitivity study, manual tuning and automatic updating were conducted to improve Model 1.

SENSITIVITY STUDY

The uncertain parameters for the sensitivity study were selected by applying common sense. The total number of parameters was 19 and these included: 1) supports stiffness, 2) moments of inertia of joists and main beams, 3) thicknesses, orthotropic ratios, and masses of the composite slabs, 4) thickness, orthotropic ratio, and mass of the roof, and 5) Young's modulus and mass of the exterior walls. In addition, parameter numbers, parameter types (characteristics), IDs of the elements in which characteristics were varied (element IDs are defined in Fig. 2), lower and upper variation bounds (given as a percentage of the starting value), and starting values of the parameters are presented in Table 2. In this table, *K* refers to stiffness, IY to moment of inertia about Y axis, THK to thickness, EX/EY to orthotropic ratio, M to mass per m^2, and E to Young's modulus. The variation bounds of the parameters correspond to modelling uncertainties, due to simplifying assumptions and idealisations made while creating the initial FE model. Also, these bounds represent the maximum changes of the parameter values allowed during the manual and automatic model updating processes.

The results of the sensitivity analysis for the four relevant modes are shown in Fig. 11(a). The

Table 2 Parameters selected for sensitivity study - Model 1

Parameter		Element ID	Boundary [%]		Starting value	Unit
No.	Type		Lower	Upper		
1	K	01	-	-	1.00E+07	N/m
2	IY	03	-25	+25	1.04E-04	m^4
3	IY	06	-25	+25	6.04E-06	m^4
4	THK	09	-25	+25	2.27E-02	m
5	EX/EY	09	-25	+25	1.36E+00	-
6	M	09	-10	+10	1.04E+02	kg/m^2
7	IY	04	-25	+25	7.46E-04	m^4
8	IY	07	-25	+25	6.04E-06	m^4
9	THK	10	-25	+25	2.27E-02	m
10	EX/EY	10	-25	+25	1.36E+00	-
11	M	10	-10	+10	1.21E+02	kg/m^2
12	E	12	-25	+25	1.10E+10	N/m^2
13	E	13	-25	+25	1.10E+10	N/m^2
14	M	12, 13	-10	+10	1.86E+01	kg/m^2
15	IY	05	-25	+25	1.30E-04	m^4
16	IY	08	-25	+25	4.50E-07	m^4
17	THK	11	-25	+25	3.30E-02	m
18	EX/EY	11	-25	+25	1.90E+00	-
19	M	11	-10	+10	1.45E+01	kg/m^2

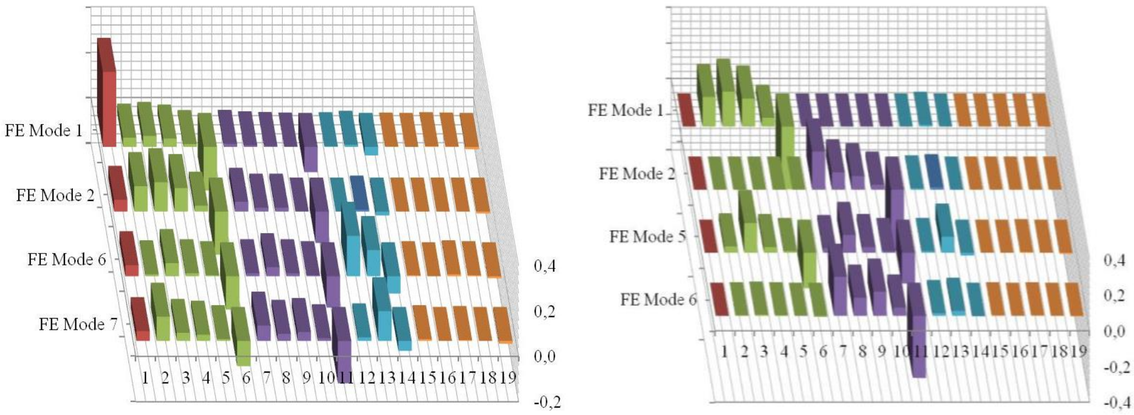

(a) Model 1 with flexible supports (b) Model 1 with rigid supports

Fig. 11 Sensitivity of the calculated natural frequencies to 1% increase in the values of each of the 19 selected updating parameters

numbers at the horizontal axis in Fig. 11(a) correspond to the parameter numbers in Table 2. It can be seen that roof properties (parameters 15-19) do have almost no influence on the four relevant modes. Surprisingly, the second FE mode, i.e., the fundamental mode of the first floor, is mostly affected by the ground floor characteristics (parameters 2-6) and to a smaller extent by the parameters of the first floor (parameters 7-11).

Further analysis has shown that an increase of the support stiffness (*K*, ID01) reduces the global motion of the whole building and confines vibrations to individual floors only. When the support stiffness value was increased to 10^{15} N/m, vibrations of the first calculated mode have engaged only the ground floor, and the second FE mode engaged only the first floor. The sequence of the higher modes changed, so the sixth FE mode (Fig. 10) became the fifth and the seventh FE mode became the sixth mode. Accordingly, vibrations of the sixth computed mode were confined to the first floor. Only the fifth FE mode kept the global character engaging both the ground and the first floor. That is a consequence of the same stiffness of these floors in the transverse direction. Furthermore, the results of the sensitivity study for the structure with fixed supports, depicted in Fig. 11(b), show that the natural frequency of the certain mode is affected only by parameters pertinent to the floor that is engaged.

MANUAL TUNING AND AUTOMATIC UPDATING

Improvement of the initial Model 1 was done using the manual tuning and automatic updating techniques described in Section 5.2. The total number of updating parameters was 11 (Table 3) and these varied in the range of ±25%, except the mass, which was varied in the range of ±10%. The convergence in the automatic updating could not be achieved, despite the fact that the majority of varied parameters were changed as much as the allowed maximum (25% or 10%, depending on the parameter). Parameter changes made during the updating process are given in Table 3, while the natural frequencies and MAC values for the updated Model 1 are listed in Table 4. The sequence of FE modes is same as for initial Model 1 (Fig. 10).

It can be seen that, although the FE model managed to capture the main features of the first four measured modes, natural frequencies of the sixth and the seventh computed mode (Table 4)

Table 3 Change of parameters selected for manual and automatic updating of Model 1

Parameter		Element ID	Value		Change [%]	Unit
No.	Type		Starting	Final		
1	K	01	1.00E+07	9.79E+06	- 2.07	N/m
2	IY	03	1.04E-04	7.83E-05	- 25.00	m^4
3	IY	06	6.04E-06	4.53E-06	- 25.00	m^4
4	THK	09	2.27E-02	1.71E-02	- 25.00	m
5	M	09	1.04E+02	1.15E+02	+ 10.00	kg/m^2
6	IY	04	7.46E-04	5.59E-04	- 25.00	m^4
7	IY	07	6.04E-06	4.53E-06	- 25.00	m^4
8	THK	10	2.27E-02	1.71E-02	- 25.00	m
9	M	10	1.21E+02	1.34E+02	+ 10.00	kg/m^2
10	E	12	1.10E+10	8.22E+09	- 25.00	N/m^2
11	E	13	1.10E+10	8.22E+09	- 25.00	N/m^2

Table 4 Comparison of numerical and experimental natural frequencies after manual and automatic updating of Model 1 and Model 2

Updated Model 1					
Mode No.	FEA [Hz]	Mode No.	EMA [Hz]	Difference [%]	MAC [%]
1	6.77	1	7.43	- 8.9	73.3
2	9.88	2	9.41	+ 5.0	78.3
6	19.64	3	16.26	+ 20.8	82.0
7	21.59	4	19.24	+ 12.2	87.9
Updated Model 2					
Mode No.	FEA [Hz]	Mode No.	EMA [Hz]	Difference [%]	MAC [%]
1	7.43	1	7.43	0.0	90.6
2	9.39	2	9.41	0.2	97.8
5	16.26	3	16.26	0.0	94.4
6	19.28	4	19.24	0.2	92.4

remained considerably high relative to the test results. MAC values for all modes were acceptable, i.e., above 70%, implying that the modes were correctly paired. The results indicate that FE model adjustment would be needed, meaning significant changes in the assumptions about the nature of the connections in the FE model of the CFS floor.

5.5.2 Improved FE model - Model 2

The joints were recognised as a potentially significant source of error in the modelling. That is why refinement of the structural model was carried out by introducing the semi-rigid moment-resisting joints at the joist-to-main beam and the main beam-to-column connections (Fig. 12). In addition, the partial interaction between the composite slab and supporting steel frame was assumed. The rationale for this modification has been that the vibration response amplitudes of lightweight floors are generally greater than those in normal floors and perhaps the friction in the joints could be overcome due to higher strains yielding semi-rigid behaviour of the connections.

A semi-rigid moment-resisting joint was modelled to provide partial rotation at the ends of the connected structural joists/beams only in the vertical plane (Fig. 12, Detail A). The stiffness of the rotational spring was introduced in Model 2 as a parameter to enable its variation later in the manual tuning and automatic updating processes. The 12×12 matrix defined for MATRIX27, which represented the main beam-to-column joints, is depicted in Fig. 9. It can be seen that only coefficients related to global ROTX degree of freedom are parameters (variable C). In the case of joist-to-main beam joints, only coefficients related to the global ROTY degree of freedom were defined by an updating parameter. Since the nodes of MATRIX27 were coincident, the global coordinate system was used for the definition of the DOFs.

Partial interaction between the composite slab and the underlying main beams/joists was simulated by introducing the semi-rigid shear connectors in the *X* and *Y* directions of the global coordinate system (Fig. 12, Detail A). MATRIX27 with coincident nodes was used to model these springs. The stiffness of the springs in the *X* and *Y* directions (coefficients that correspond to UX and UY in the element matrix) was introduced as a parameter, to allow for its variation in the

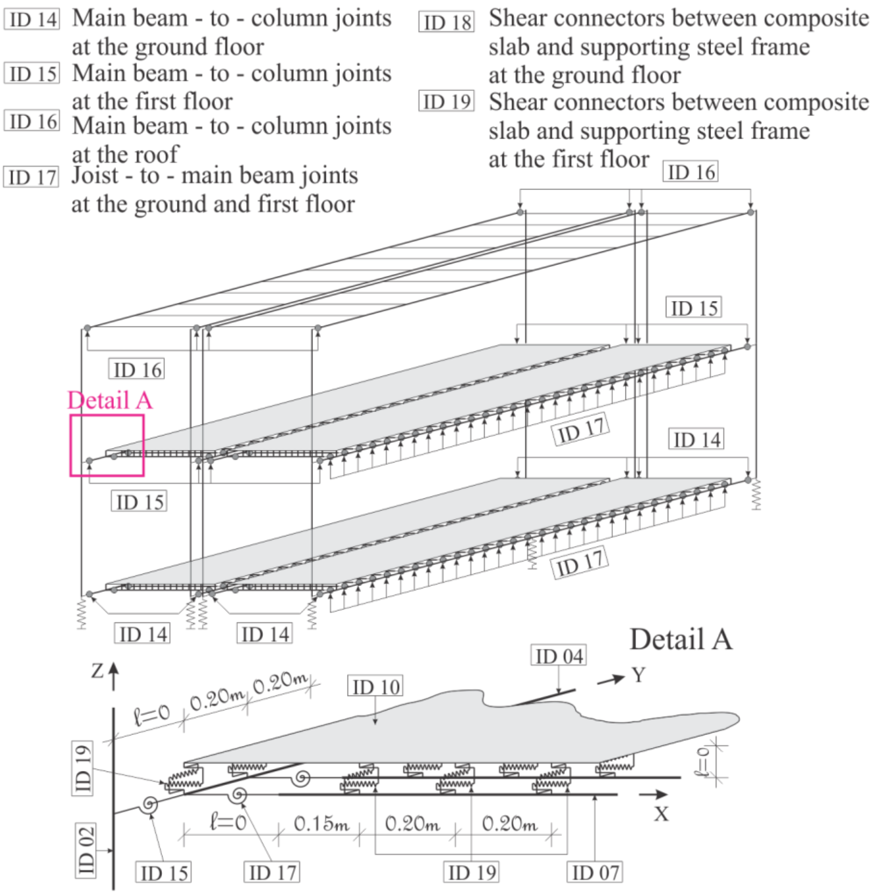

Fig. 12 Structural scheme used for the development of Model 2 featuring main beam-to-column and joist-to-main beam semi-rigid joints

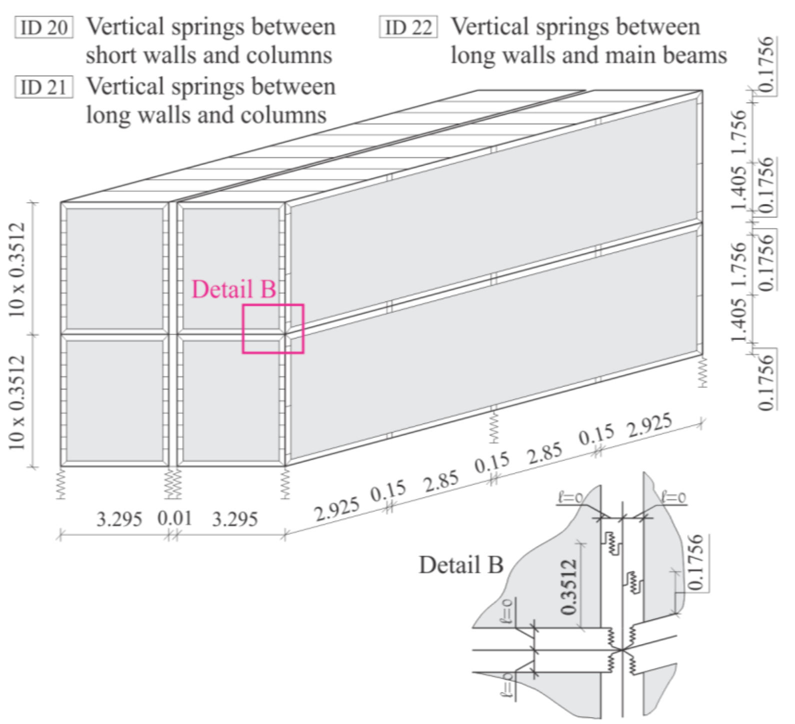

Fig. 13 Structural scheme used for the development of Model 2 with façade walls-to-structural frame semi-rigid connections added

subsequent model updating process. The neutral axes for the slab and the main beams/joists are separated when the partial interaction is assumed, and their positions depend on the stiffness of the shear connectors. Moments of inertia of the main beams/joists about these neutral axes were calculated following a published procedure (EN 1995-1-1:2004, Annex B).

Also, it was decided to model more realistically the way the façade walls were connected to the structural frame. According to the technical drawings, short façade walls (ID12) were connected only to the columns by self-tapping screws. Long façade walls (ID13) were attached to the columns and main beams by bolts. Thus, the walls in the FE model were connected to the structural frame by springs that represented the screws and bolts (Fig. 13). Bearing in mind that the horizontal displacements of the walls were fully restrained in the model, the springs were employed to simulate the sliding in the vertical direction between the walls and the structural frame (Fig. 13, Detail B). This way, the façade wall was decoupled from the structural frame. This, in turn, reduced its own deformation, hence its contribution to the overall frame stiffness. Again, MATRIX27 was used to model such flexible connections. In this case, the coefficient related to the vertical translation (UZ) in the12x12 matrix was defined parametrically, while all the other coefficients were assumed, as previously, to be 10^{15} N/m, or 10^{15} Nm/rad.

The starting value for the rotational stiffness of the joist-to-main beam joints, i.e., the partial depth end plate joint depicted in Fig. 14(c), was calculated by implementing the *component method* (EN 1993-1-8: 2005). Main beam-to-column joints were initially assumed to be rigid, since they were made with thick end plates (Fig. 14(e)). The shear stiffness of the bolts connecting

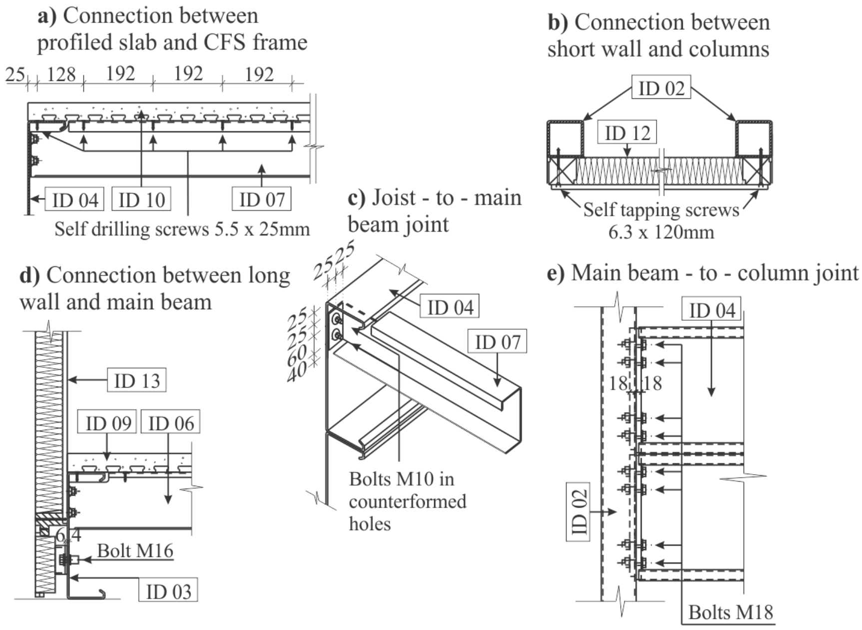

Fig. 14 Connections details

Table 5 Change of parameters selected for manual and automatic updating of Model 2

Parameter		Element ID	Boundary		Value		Unit
No.	Type		Lower	Upper	Starting	Final	
1	K	01	5.00E+06	1.00E+15	1.00E+07	2.90E+07	N/m
2	K	14	0.00E+00	1.00E+15	1.00E+15	1.00E+15	Nm/rad
3	K	15	0.00E+00	1.00E+15	1.00E+15	1.00E+15	Nm/rad
4	K	16	0.00E+00	1.00E+15	1.00E+15	1.00E+15	Nm/rad
5	K	17	0.00E+00	1.00E+15	3.00E+04	3.00E+04	Nm/rad
6	K	18	5.00E+05	1.00E+15	1.00E+06	5.65E+06	N/m
7	K	19	5.00E+05	1.00E+15	1.00E+06	3.00E+06	N/m
8	K	20	5.00E+05	1.00E+15	1.00E+06	3.12E+06	N/m
9	K	21	5.00E+05	1.00E+15	8.00E+07	2.16E+07	N/m
10	K	22	5.00E+05	1.00E+15	3.08E+07	8.32E+06	N/m

the long exterior walls to the structural frame (Fig. 14(d)) was calculated according to the method published by Zadanfarrokh and Bryan (1992). Estimation of the shear stiffness for the screws attaching the short walls to the structural frame (Fig. 14(b)) and the ones between the composite slab and the supporting steel frame (Fig. 14(a)) was difficult, due to the lack of reliable guidelines. The starting values for these parameters were adopted in the manual tuning process, through minimisation of the error function.

A sensitivity study and automatic updating of Model 2 were carried out. It was decided to vary only the stiffness values of the building supports and the connections, as they were recognised as the most uncertain parameters (Table 5). The lower bounds in Table 5 correspond to flexible behaviour of the connections and supports, while the upper bounds relate to their rigid behaviour. Rotational springs (ID14-ID17, Table 5) have the lower bound values equal to zero and the lower bound values of translational springs (ID01, ID18-ID22, Table 5) are from $5*10^5$ N/m to $5*10^6$ N/m to preserve the structural integrity. This time, the convergence was achieved. Parameter starting values and changes are given in Table 5. Natural frequencies and MAC values for updated Model 2 are presented in Table 4. It can be seen that the differences between the calculated and experimental natural frequencies are negligible for all four paired experimentally and numerically calculated modes. MAC values for all Model 2 modes increased significantly relative to Model 1, and they were remarkably high.

5.6 Interpretation of parameters in updated FE Model 2

Physical interpretation of the updated parameters is crucial for understanding the dynamic behaviour and modelling errors. Table 5 presents all uncertain parameters that were introduced in the model updating process. The starting values for the connection stiffness were calculated following procedures defined for static analysis (EN 1993-1-8: 2005, Zadanfarrokh and Bryan 1992). The rotational stiffness of the main beam-to-column joints at all three building levels (ID14 -16, Table 5) remained the same, reassuringly indicating rigid behaviour. The rotational stiffness of the joist-to-main beam joints at the ground and first floors (ID17, Table 5) was also unchanged. This type of joint, i.e., the partial end plate joint depicted in Fig. 14(c), is considered to be a pin joint in static analysis. The fact that reduction of the joint stiffness to zero would have negligible effects on the results in this study implies that the stiffness of $3*10^4$ Nm/rad (ID17, Table 5) is so small that the joint can also be considered to be a pin joint in vibration analysis. Stiffness values of all kinds of the shear connections that were introduced in the model (ID18-22, Table 5) have changed in the model updating process. The ones related to vertical springs between long façade walls and structural frame (ID21 and ID22, Table 5) were reduced to approximately 27% of their starting values, implying lower dynamic stiffness comparing to static stiffness.

The shear connectors between the composite slab and the supporting steel frame were the same at the ground and the first floors. However, stiffness values for these parameters (ID 18 and ID 19, Table 5) obtained in the model updating process are different. Bearing in mind that the stiffness of the shear connectors directly affected the moments of inertia of the slab and the main beams/joist, this result may indicate a different level of partial interaction between the floor components at the ground and first building levels.

Apparently, the introduction of the semi-rigid connections was crucial for achieving good agreement between the numerical and experimental results. The reasons for this could be:

- strains and displacements were actually large enough to overcome friction in joints (galvanised surface of CFS profiles and fasteners yields lower friction coefficients compared to other forms of coating or bare steel (Zadanfarrokh and Bryan 1992)),
- small thickness of the CFS sheets dominates the stiffness of the connections, and
- second order effects, such as: tilting of the fastener in a hole, distortion of the thin steel sheet around the hole in tension, etc. (Sandesh and Sivakumaran 2012).

It is important to emphasise that the set of the updated parameters obtained in this exercise is not a unique solution, but it is a quite reasonable quantification of the modelling uncertainties. Also, this set provides excellent agreement between the FE model and the real structure, taking into account both natural frequencies and mode shapes. The matching of the values of the natural frequencies and mode shapes for four paired modes is probably one of the best ever reported in the literature pertinent to formal FE model updating of building floors, still yielding a very reasonable and believable set of updated uncertain parameters.

6. Conclusions

In general, the primary aims and contributions of the presented research are concerned with modal analysis of lightweight steel floors from the vibration serviceability standpoint. The proposed FE model updating procedure has a practical significance for researchers and engineers in a way that formal updating of FE models can be conducted using the design optimisation methods comprised in commercial FEM software packages, like ANSYS. The key research results are further emphasised.

The measurements presented in Section 4 indicate the appreciable contribution of the higher modes of the CFS floor to the floor vibration response. This requires the development of an FE model that would quite accurately capture not only the fundamental but also the higher vibration modes. Therefore, the lowest four modes obtained by the curve-fitting of the FRFs measured during the floor modal testing were used for the validation of the structural FE model in this paper.

It was found that the shakers placed on the first floor excited the whole tested building to vibrate in the vertical direction, indicating the presence of global building modes. This fact was decisive to develop the initial FE model of the whole building and not only of the first floor. The sensitivity study in Section 5.3.1 indicated that the flexible building supports caused an interaction between the building levels in every mode.

The initial FE model of the tested building was developed according to recommendations that are common in civil structural engineering practice. However, the differences between the measured and FE-calculated natural frequencies were up to 41%. Considerable improvement of the FE model was realised by manual tuning and automatic updating techniques, using the design optimisation module of the ANSYS FE code. A crucial improvement of the initial FE model was its adjustment, by introducing a partial interaction between the composite slab and supporting main beams/joists and by incorporating the semi-rigid moment-resisting joints along the ground floor and the first floor edges.

The non-structural exterior walls were incorporated in the structural FE model, due to their evident restraining effect on the floor edges in the vertical direction, which was observed in the experimentally estimated mode shapes. However, explicitly modelled walls not featuring adjusted properties of the cross sections and rigid connections, introduced too much stiffness to the FE model. That is why the decision was taken to reduce their effects by inserting the semi-rigid connections, i.e., vertical springs, between the walls and the structural frame.

Finally, the adjusted and then updated model featuring semi-rigid connections led to markedly improved results. The first four natural frequencies matched ideally and all MAC values were above 90%. The introduction of the flexible supports and more realistic modelling of the floor boundary conditions, as well as non-structural façade walls, proved to be crucial in the development of the new, more successful, modelling strategy. The process used to develop the 10 identified and fully updated FE modelling parameters is based on published information and parameter adjustment resulting from FE model updating. This can be utilised for future design of similar lightweight steel floors in prefabricated buildings when checking their vibration serviceability, likely to be their governing design criterion.

Acknowledgements

This research has been supported by the Serbian Ministry of Education, Science, and Technological Development, Project Ref. TR36023 and TR37014, and by the UK Engineering and Physical Sciences Research Council (EPSRC) Platform Grant Ref. EP/G061130/2. Special thanks go to Portakabin Ltd who also partly funded this work and provided us with the unique test structure, technical information and assistance during testing.

References

Allemang, R.J. and Brown, D.L. (1982), "A correlation coefficient for modal vector analysis", *Proceedings of the 1st International Modal Analysis Conference (IMAC)*, Orlando, FL, USA, November.

Allen, D.E., Onysko, D.M. and Murray, T.M. (1999), *ATC Design Guide 1: Minimizing Floor Vibration*, Applied Technology Council, Redwood, CA, USA.

Ansys Inc. (2005), Release 10.0, Documentation for ANSYS, Ansys Inc., Canonsburg.

Brownjohn, J.M.W. and Xia, P. (2000), "Dynamic assessment of curved cable-stayed bridge by model updating", *J. Struct. Eng.*, ASCE, **126**(2), 252 -260.

Chui, Y.H. (1988), "A rational method of evaluating the dynamic response of timber floors", *Struct. Eng. Rev.*, **1**(1), 151-164.

Cowles, E. and Warner, P. (2013), *Prefabrication and Modularization in Construction*, FMI Corporation, Raleigh, NC, USA.

Egan, J. (1998), *Rethinking Construction: Report of the Construction Task Force*, HMSO, London, UK.

El-Dardiry, E. and Ji, T. (2006), "Modelling of the dynamic behaviour of profiled composite floors", *Eng. Struct.*, **28**(4), 567-579.

El-Dardiry, E. and Ji, T. (2007), "The effect of eccentricity on the free vibration of composite floors", *Compos. Struct.*, **85**(21-22), 1647-1660.

EN 1993-1-8 (2005), *Eurocode 3: Design of Steel Structures-Part 1-8: Design of Joints*, European Committee for Standardization, Brussels, Belgium.

EN 1995-1-1 (2004), *Eurocode 5: Design of Timber Structures-Part 1-1: General-Common Rules and Rules for Buildings. Annex B*, European Committee for Standardization, Brussels, Belgium.

Ewins, D.J. (2000), *Modal Testing: Theory, Practice and Application*, Research Studies Press Ltd., Baldock, Hertfordshire, UK.

Filiatrault, A., Folz, B. and Foschi, R.O. (1990), "Finite-strip free-vibration analysis of wood floors", *J. Struct. Eng.*, ASCE, **116**(8), 2127-2142.

Friswell, M.I. and Mottershead, J.E. (1995), *Finite Element Model Updating in Structural Dynamics*, Kluwer Academic Publishers, Dordrecht, Netherlands.

Gupta, A. (1985), "Reliability of floors under impact vibrations", M.A.Sc. Dissertation, The University of British Columbia, Vancouver, Canada.

Hartley, A. and Blagden, A. (2007), "Current practices and future potential in modern methods of construction", Report No. WAS003-001, Waste and Resources Action Programme, Banbury, Oxon, UK.

Hu, L.J. (1992), "Prediction of vibration responses of ribbed plates by modal synthesis", Ph.D. Dissertation, The University of New Brunswick, Fredericton, NB, Canada.

Hu, L.J., Chui, Y.H. and Jiang, L. (2002), "Verification of a finite element model for wood-based floor structures with lateral reinforcements", *Proceedings of the 7th World Conference on Timber Engineering*, Shah Alam, Malaysia, August.

Hu, L.J., Desjardins, R. and Chui, Y.H. (2006), "Nature of vibrations induced by footsteps in lightweight and heavyweight floors", *Proceedings of the 9th World Conference on Timber Engineering*, Portland, OR, USA, August.

IBC (2012), *International Building Code,* International Code Council, Inc.

Jiang, L., Hu, L.J. and Chui, Y.H. (2004), "Finite-element model for wood-based floors with lateral reinforcements", *J. Struct. Eng.*, ASCE , **130**(7), 1097-1107.

Kesti, J., Hicks, S., Rackham, J., Widman, J., Villot, M., Guigou, C., Rodriguez-Ferran, A., Poblet-Puig, J., Sipari, P., Talja, A., Ljunggren, F. and Agren, A. (2008), "High quality acoustic and vibration performance of lightweight steel constructions", Contract No. RFSR-CT-2003-00025, Office for Official Publications of the European Communities, Luxembourg.

Kraus, C.A. (1997), "Floor vibration design criterion for cold-formed C-shaped supported residential floor systems", M.Sc. Dissertation, Faculty of the Virginia Polytechnic Institute and State University, Blacksburg, VA, USA.

Lawson, R.M., Grubb, P.J., Prewer, J. and Trebilcock, P.J. (1999), *Modular Construction Using Light Steel Framing: An Architect's Guide,* SCI-P-272, The Steel Construction Institute, Berkshire, UK.

Leichti, R.J., Hyde, R.A., French, M.L. and Camillos, S.G. (2000), "The continuum of connection rigidity in timber structures", *Wood and Fiber Science,* **32**(1), 11-19.

Ljunggren, F. (2006), "Floor vibration: Dynamic properties and subjective perception", Ph.D. Dissertation, Lulea University of Technology, Lulea, Sweden.

Mehta, M., Scarborough, W. and Armpriest, D. (2013), "Cold-formed (light-gauge) steel construction", *Building Construction-Principles, Materials, and Systems*, 2nd Edition, Pearson Education Inc., New Jersey, USA.

National Research Council (NRC) (2009), *Advancing the Competitiveness and Efficiency of the U.S. Construction Industry,* National Academy of Sciences, Washington, USA.

Ohlsson, S.V. (1982), "Floor vibrations and human discomfort", Ph.D. Dissertation, Chalmers University of Technology, Gothenburg, Sweden.

Parnell, R.A. (2008), "Vibration serviceability and dynamic modeling of cold-formed steel floor systems", M.A.Sc. Dissertation, University of Waterloo, Ontario, Canada.

Parnell, R.A., Davis, B.W. and Xu, L. (2010), "Vibration performance of lightweight cold-formed steel floors", *J. Struct. Eng.*, ASCE, **136**(6), 645-653.

Pavic, A. and Reynolds, P. (2002), "Vibration serviceability of long-span concrete building floors. Part 2: Review of mathematical modelling approaches", *Shock Vib. Dig.*, **34**(4), 279 -297.

Pavic, A. and Willford, M. (2005), "Appendix G: Vibration serviceability of post-tensioned concrete floors" *Post-Tensioned Concrete Floors: Design Handbook*, Technical Report 43, Concrete Society, Slough, UK.

Pavic, A., Miskovic, Z. and Zivanovic, S. (2008), "Modal properties of beam-and-block pre-cast floors", *IES J. Part A: Civil Struct. Eng*., **1**(3), 171-185.

Rack, W. and Lange, J. (2009), "Human induced vibrations of lightweight steel floor systems", *Proceedings of the 11th Nordic Steel Construction Conference*, Malmo, Sweden, September.

Reynolds, P. and Pavic, A. (2000), "Quality assurance procedures for the modal testing of building floor structures", *Exp. Tech.*, **24**(4), 36-41.

Reynolds, T., Harris, R. and Chang, W.S. (2014), "Stiffness of dowel-type timber connections under pre-yield oscillating loads", *Eng. Struct.*, **65**, 21-29.

Sandesh, R.A. and Sivakumaran, K.S. (2012), "Finite element models for thin-walled steel member connections", *ISRN Civ. Eng.*, Vol. 2012, Article ID 197170, DOI: 10.5402/2012/197170.

Sinha, J.K. and Friswell, M.I. (2002), "Model updating: A tool for reliable modelling, design modification and diagnosis", *Shock Vib. Dig.*, **34** (1), 27-35.

Tangorra, F.M., Xu, L. and Xie, W.C. (2002), "Vibration characteristics of lightweight floors using cold-formed steel joist", *Proceedings of the 16th International Specialty Conference on Cold-Formed Steel Structures,* Orlando, FL, USA, October.

Timetric (2014), *The Global Prefabricated Buildings Market - Key Trends and Opportunities to 2017*. Timetric, London, UK.

https://timetric.com/research/report/cn0135sr--the-global-prefabricated-buildings-market-key-trends-and-opportunities-to-2017/

Vibrant Technology (2003), *ME'Scope VES Operating Manual*, Vibrant Technology, Scotts Valley, CA,

USA.
Willford, M.R. and Young, P. (2006), *A Design Guide for Footfall Induced Vibrations of Structures*, CCIP-016, The Concrete Centre, Blackwater, Camberley, Surrey, UK.
Wyatt, T.A. (1989), *Design Guide on the Vibration of Floors*, SCI-P-076, The Steel Construction Institute, Berkshire, UK.
Xu, L. and Tangorra, F.M. (2007), “Experimental investigation of lightweight residential floors supported by cold-formed steel C-shape joists”, *J. Constr. Steel Res.*, **63**(3), 422-435.
Xu, L. (2011), “Floor vibration in lightweight cold-formed steel framing”, *Adv. Struct. Eng.*, **14**(4), 659-672.
Zadanfarrokh, F. and Bryan, E.R. (1992), “Testing and design of bolted connections in cold formed steel sections”, *Proceedings of the 11th International Specialty Conference on Cold-Formed Steel Structures,* Saint Louis, MO, USA, October.
Zhao, X.L., Taplin, G. and Alikhail, M. (2003), “Connection stiffness and natural frequency of DuraGal lightweight floor systems”, *Struct. Eng. Mech.*, **15**(3), 269-284.
Zhou, X., He, Y., Jia, Z. and Nie, S. (2011), “Experimental study on vibration behaviour of cold-form steel concrete composite floor”, *Adv. Steel Constr.*, **7**(3), 302-312.

CC